Drug Development and Industrial Pharmacy, 2010; 36(8): 993–1004

informa
healthcare

ORIGINAL ARTICLE

Investigation on the synergistic effect of a combination of chemical enhancers and modulated iontophoresis for transdermal delivery of insulin

Rachna Rastogi[1,2], Sneh Anand[1,2], Amit K. Dinda[3] and Veena Koul[1,2]

[1]Centre for Biomedical Engineering, Indian Institute of Technology, Hauz Khas, New Delhi, India, [2]Biomedical Engineering Unit, All India Institute of Medical Sciences, New Delhi, India and [3]Department of Pathology, All India Institute of Medical Sciences, New Delhi, India

Abstract

Purpose: The main objective of this study was to assess the flux enhancement of insulin transdermally by utilizing a complex of chemical enhancers in combination with modulated iontophoresis. *Methods*: The experiments were performed on porcine epidermis model under three different circumstances, namely, (a) 1-hour modulated iontophoresis alone; (b) pretreatment with vehicle and chemical enhancer combinations and (c) combination of (a) and (b). The mechanism of action of the enhancers was studied using infra-red spectra by derivative and curve-fitting techniques and Confocal laser scanning microscopy. The efficacy of the optimized combination was tested in vivo in streptozocin-diabetic Wistar rats. *Results*: A blend of 1,8 cineole, oleic acid and sodium deoxycholate in propylene glycol : ethanol (7:3) resulted in 45% enhancement, when permeation was performed in combination with iontophoresis as compared to the latter alone. In-depth analysis of infra-red spectra revealed that each of the enhancers acted differentially on lipid-protein domains of the stratum corneum thereby supporting the observed synergism. Movement of fluorescently labeled insulin depicted highlighted follicular regions and paracellular accumulation of the probe after iontophoresis and chemical enhancer treatment respectively. Presence of the fluorescent peptide in these regions 4 hour after treatment with the combination reinforced the results of the permeation studies. Finally the combination of modulated iontophoresis with chemical enhancer blend resulted in lowering of blood glucose for 8 hour in vivo. *Conclusions*: The study proved the applicability of modulated iontophoresis with chemical pretreatment in delivering insulin transdermally.

Key words: *Chemical enhancers; confocal microscopy; in vivo evaluation; insulin; second-derivative FTIR; transdermal iontophoresis*

Introduction

Development of facile routes for bioengineering of proteins and oligonucleotides has widened the realm of molecules used as therapeutic agents. However, the administration of these molecules is limited to the parenteral route and has not been given much attention. Delivery through the oral route is limited by the pH fluctuations and enzymatic activity in the GI tract, which inactivate such 'sensitive' molecules. Transdermal delivery is an exciting option because the skin offers a large surface area and has relatively fewer enzymes. The limitation to this is the formidable barrier posed by the 'brick and mortar' arrangement of the stratum corneum (SC). The 500 Dalton rule limits the movement of molecules to some lipophilic, neutral, or uncharged molecules that are suitable for transdermal delivery. Candidates such as proteins that are charged and hydrophilic in nature with high molecular weights ranging in thousands of daltons require some external assistance to aid their movement across the skin[1]. Application of chemical enhancers and/or physical agents such as current (iontophoresis), high voltage (electroporation), radiofrequency, ultrasound (sonophoresis), and microneedles[2] has been studied to modify the barrier properties. Many chemicals have been evaluated as penetration enhancers;

Address for correspondence: Dr. Veena Koul, Centre for Biomedical Engineering, Indian Institute of Technology, II/192, Hauz Khas, New Delhi 110 016, India. Tel: +91 11 26591041, Fax: +91 11 26592037. E-mail: veenak_iitd@yahoo.com

(Received 25 Nov 2009; accepted 5 Feb 2010)

ISSN 0363-9045 print/ISSN 1520-5762 online
DOI: 10.3109/03639041003682012

however, their enhancement potential is dependent on the physicochemical properties of the molecule of concern. Similarly, various physical enhancement methods have been investigated; however, most technologies are in the stage of development or clinical trials.

Diabetes mellitus (DM) has been stated as the 'most common noncommunicable diseases' globally. The World Health Organization has proclaimed the disease as the fourth or fifth leading cause of death in most developed countries and as an epidemic in many developing countries[3,4]. Although noninsulin-dependent DM (NIDDM; Type II) accounts for nearly 90–95% of the diabetic population, the incidence of childhood onset DM or Type I is being estimated to have an overall annual growth of around 3% with a major contribution of nearly 25% from the South-East Asian region[5].

Although enormous research has been carried out[6,7], a clinically acceptable protocol for transdermal delivery of insulin has not yet been developed. The variations in the results are due to skin permeability and metabolic activity differences among the animal species used for experiments, lack of data on cadaver epidermis or relevant skin types such as porcine ear flap model, and experimental protocols of prolonged iontophoretic and chemical pretreatment durations ranging in hours. These issues have been the driving force in developing a transdermal-based therapeutic system for insulin delivery.

The main objective of this study was to design a therapy comprising chemical enhancers and iontophoresis for the transport of insulin so that it is clinically acceptable. Iontophoresis involves the delivery of low-intensity current for a prolonged duration to lower the epidermal resistance thereby facilitating the movement of molecules across the SC. This technique is FDA approved and is being applied for the delivery of lidocaine and fentanyl. Extensive screening of most commonly reported GRAS enhancers from the classes of alcohols, bile salts, fatty acids, and terpenes was carried out to formulate a blend that would result in maximum permeation enhancement. The mechanism of enhancement by enhancer combination was studied by curve-fitting analysis of lipid and amide I vibrations of treated cadaver SC by infrared spectroscopy. To further confirm the findings of the permeation studies, the movement of fluorescently labeled insulin was tracked in cadaver epidermis. Finally, the efficacy of the developed protocol was tested in streptozocin (STZ)-diabetic Wistar rat model.

Materials and methods

Chemicals

Insulin, human recombinant (expressed in *Escherichia coli*, F.W. 5807.6 Da; 28.6 USP units/mg), fluorescein isothiocyanate FITC-labeled bovine insulin (FITC-BI; from bovine pancreas with FITC content 1.3 mol/mol insulin), and STZ were purchased from Sigma-Aldrich (St. Louis, MO, USA). Terpenes and fatty acids were purchased from Acros Organics (Geel, Belgium). Polyvinyl alcohol (PVA; MW 1,25,000, 88% hydrolysis), glycine, and sodium deoxycholate were obtained from CDH Laboratories (Mumbai, India). Glutaraldehyde (25% aqueous solution) was procured from Thomas Baker (Mumbai, India). All chemicals and reagents used were of analytical grade and were used as received.

Skin preparation for permeation studies

Porcine epidermis was prepared by trypsin digestion method from pig ears obtained from the local abattoir for in vitro permeation studies. The whole skin from the dorsal side was separated from the underlying cartilage and was floated on 0.15% trypsin solution for 4 hours with the SC side facing upward. The thickness of the prepared sample ranged from 300 to 500 μm. The samples were dried, stored at −20°C, and used within a week. The membranes were rehydrated in phosphate-buffered saline (PBS) pH 7.4 before use.

Cadaver skin (aged = 20–40 years; either sex) for confocal microscopy was obtained from the mortuary after the approval from the Institutional Ethical Committee. Epidermis was prepared by heat separation method by placing full thickness skin in water at 60°C for 1 minute, the epidermis teased off carefully, washed, and stored at −20°C until use[8].

Preparation of hydrogels

Ten percent aqueous solution of PVA was cross-linked at 35°C for 8 hours with aqueous solution of glutaraldehyde (equivalent to 2.5 wt.%) to prepare hydrogels. The gels were washed to remove unreacted glutaraldehyde, endcapped with 0.2 M glycine solution, and lyophilized (Freezone, Labconco, Kansas City, MO, USA) for 10 hours at −80°C. Residual PVA was determined by a colorimetric method based on the formation of a complex between two adjacent hydroxyl groups of PVA and an iodine molecule[9]. To 0.5 mL of the washings, 3 mL of 0.65 M solution of boric acid and 0.5 mL of a solution of I_2/KI (0.05/0.25 M) were added and the volume was made up to 10 mL. The absorbance was measured at 600 nm after 15 minutes of incubation. Percent unreacted PVA was determined as follows:

$$\text{Percent residual PVA} = \frac{\text{Amount of PVA in solution}}{\text{Total PVA content in hydrogel}} \times 100.$$

Swelling studies of the above-prepared hydrogels were carried out in 0.1 N HCl and PBS pH 7.4 containing 0.0025% sodium azide at 37°C. Percent swelling is given by

$$\text{Percent swelling} = \frac{W_s - W_d}{W_d} \times 100,$$

where W_s = weight of the swollen hydrogel and W_d = initial weight of the dried hydrogel.

Two milligram of insulin, equivalent to 57.2 IU (10 mg/mL solution in citrate buffer pH 3.5), was loaded by dropping 200 µL of insulin solution onto each lyophilized patch before the study. This method was selected over the conventional dipping technique wherein the dried hydrogels are placed in drug solution and allowed to swell to avoid drug wastage as well as to ensure uniform content in all the patches.

To understand the suitability of the prepared hydrogel as a reservoir, insulin release from the formulation was studied in PBS pH 7.4. The hydrogel (2 mg/disc insulin content) was dipped in 1 mL of PBS pH 7.4 at 37°C and insulin release was monitored for 8 hours. The insulin concentration was determined by a solid-phase two-site immunoassay (Human Insulin Kit, Mercodia, Uppsala, Sweden). The test is based on direct sandwich technique consisting of two monoclonal antibodies directed against separate antigenic determinants on insulin.

In vitro studies

Permeation studies were carried out using unjacketed Franz diffusion cells (diffusion area 1.54 cm^2) placed on a magnetic stirrer (Remi 2ML, Mumbai, India) at 37 ± 0.5°C. Ten milliliters of PBS pH 7.4 containing urea (2 mg/mL) and sodium azide (0.0025%) was used as the receptor medium for the studies. Urea is known to prevent aggregation of insulin thereby preventing its inactivation[10]. Rehydrated porcine epidermis was equilibrated for 1 hour with constant stirring. Modulated DC (mDC) iontophoresis was carried out by an in-house developed system (Figure 1)[11]. 0.5 mA/cm^2 of current of 1 kHz was delivered through a thin gold plate (diffusion area = 1.54 cm^2 and thickness 0.5 mm) anode and a gold wire cathode inserted in the arm of the receptor compartment. The hydrogel reservoir was placed on the donor side of the diffusion cell sandwiched between the SC and the gold electrode. Aliquots were withdrawn from the receptor solution and replaced with fresh medium. The cumulative amount of insulin permeated per unit skin surface area was plotted against time and the slope of the linear portion of the plot was estimated as the steady-state flux (J), which is represented by the following equation:

$$J = \frac{\Delta Q_t}{A\Delta t}, \quad (1)$$

where Q_t is the amount of solute transported across membrane, t is time, and A is the exposed area of the membrane for diffusion. The permeability coefficient, K, was calculated as follows[12]:

$$K = \frac{J}{C_i}, \quad (2)$$

where C_i is the concentration of insulin in the donor chamber.

Insulin concentration was determined by ELISA method as reported above.

Chemical pretreatment

The effect of pretreatment with GRAS chemical penetration enhancers (CPEs) of various classes such as alcohols, terpenes, fatty acids, and bile salts on insulin permeation was studied. One hundred microliters of

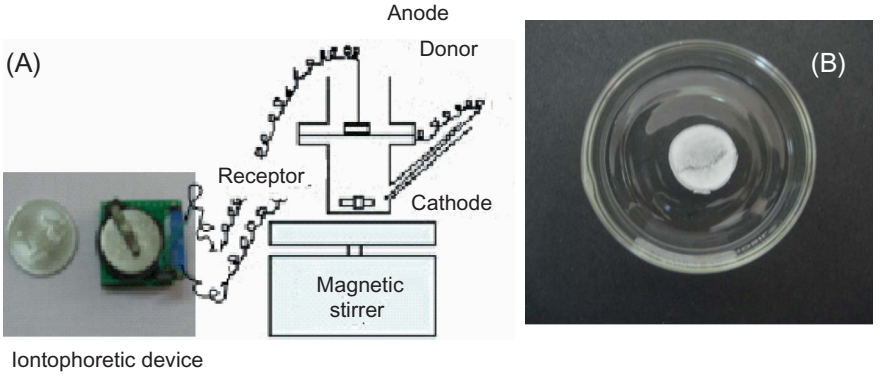

Figure 1. (A) Schematic representation of the developed modulated DC iontophoretic system and experimental setup (Drawing not to scale), and (B) image of prepared PVA hydrogel patch.

solvents or 5% ethanolic solutions of CPEs were applied on the SC after equilibration. The treated area was air-dried for 2 minutes before placement of the hydrogel patch for passive and iontophoretic studies.

Attenuated total reflectance-Fourier transform infrared spectroscopy

Fourier transform infrared (FTIR) spectra of cadaver SC were collected in the frequency range of 4000–650 cm^{-1} (Spectrum One, Perkin Elmer, CT, USA) with zinc sulfide as internal reflection element at 60° incident angle. The spectra were taken before and after chemical enhancer treatment in triplicate; each sample thus served as its control. All spectra reported are an average of 64 scans (data collection time was 120 seconds) with a resolution of 2 cm^{-1}, Fourier-transformed and ratioed against a background interferogram. Second derivative of the amide I band of proteins was determined with 13-point smoothing to remove the noise. Gaussian curve-fitting of the inverted second-derivative spectra was carried out by Origin 6.1 software (Originlab Corporation, Northampton, MA, USA). The fraction of the components was determined by computing the area of the component peak divided by the sum of the areas of all the components in the band.

Confocal laser-scanning microscopy

The mechanism of permeation of FITC-BI by the application of iontophoresis and chemical enhancers across cadaver epidermis was studied by confocal laser-scanning microscopy (CLSM). The microscope, Carl Zeiss LSM 510 (Germany), equipped with an Argon laser (488 nm) was used to excite the fluorophore. The samples were mounted inverted onto the platform with the SC side facing the objective lens system (Plan Neofluar 20 × /0.5) and 50–90% laser intensity. FITC-BI was detected by a low pass filter of wavelength 505 nm. Optical sectioning was done parallel to the *xy* plane of the skin surface. The point $z = 0$ was fixed for all the samples to assess the depth of penetration of the fluorescent probe into the epidermis. All the images were obtained at the same pinhole aperture, filter, lens, and scan speed with an average of 8 scans per image.

In vivo delivery of insulin

Male adult Wistar rats (200–250 g) were selected for the study. The animals were fasted for 16 hours with free access to water before the experiment. DM was induced by an intraperitoneal (i.p.) injection of 45 mg/kg of STZ in citrate buffer pH 4.5 in fasted animals under light ether anesthesia[13]. The buffer was mixed to STZ just before injection. The body weight and blood glucose levels of the animals were monitored regularly for the complete duration. Animals with percent blood glucose levels (%BGL) above 200% were included in the study.

The treatment groups include

- diabetic control (normal saline intravenous),
- insulin subcutaneous s.c. (s.c. injection of 30 IU/kg body weight),
- insulin I (1 hour mDC iontophoresis), and
- insulin IC (pretreatment with enhancer combination + 1-hour mDC iontophoresis).

Rats were administered with ketamine intramuscularly (60 mg/kg) 15 minutes before the start of the experiments. Subcutaneous (s.c.) insulin (5–7 IU) was injected in control animals for comparison. One hundred microliter enhancer combination was applied onto the cleaned areas and air-dried. Thereafter, PVA hydrogel containing insulin (~2 mg) and the anode was placed. A normal saline-loaded disc was placed beneath the cathode. The gels and the electrodes were held in place by coated adhesive tapes. After 1 hour of mDC iontophoresis, the area was occluded by coated adhesive tapes to avoid drying of the gel. 0.1 mL blood was withdrawn from the tail vein at regular time intervals following administration for the estimation of blood glucose. All results expressed are a mean of at least six animals. Blood glucose was determined using Ascensia kit (Bayer Healthcare, Tarrytown, NY, USA; range = 10–550 mg/dL).

Data treatment

All the results were expressed as mean ± SD (n = 3–5 for in vitro and 6 for in vivo studies) and statistically analyzed by one-way ANOVA with post-test (Graphpad Prism, La Jolla, CA, USA). The level of significance was taken as $P < 0.05$.

Results

PVA cross-linked with 2.5 wt.% glutaraldehyde was found to give sufficiently firm and flexible hydrogel patches (Figure 1), which showed good swelling properties (325.6% and 413% in PBS pH 7.4 and 0.1 N HCl, respectively) and drug release behavior (89.07 ± 0.359% in 8 hours). The residual PVA content was less than 0.5% after 8 hours suggesting nearly complete cross-linking.

Peptide delivery by mDC iontophoresis is not substantial

Porcine ear epidermis is considered a closer model to human skin because of similarity in morphology and permeability characteristics, and thus was used in this

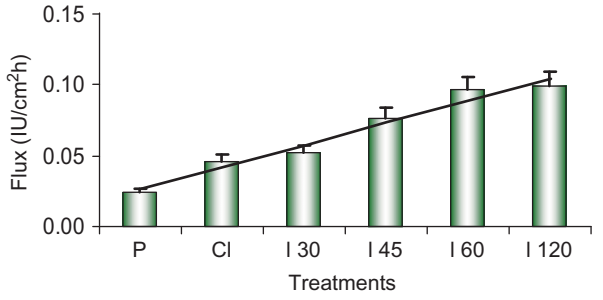

Figure 2. Comparison of insulin release profile on passive application, constant and pulsed iontophoresis (0.5 mA/cm^2) at varied time intervals [P – passive, CI – constant current, I – pulsed iontophoresis for 30 minutes (I 30), 45 minutes (I 45), 60 minutes (I 60), and 120 minutes (I 120)] (n = 3–4 for all experiments).

study[14,15]. Passive diffusion of insulin across skin was found to be insignificant. As insulin has a +4 charge at pH 3.6 (pI 5.4), anodal iontophoresis was carried out at 0.5 mA/cm^2 for varied time intervals till a maximum of 2 hours. The flux was found to increase linearly till t = 60 minutes. Further increase in duration resulted in no significant alteration in the flux (P < 0.05). The application of mDC iontophoresis resulted in higher drug flux 0.096 ± 0.040 IU/cm^{2}h as compared with 0.0244 ± 0.009 IU/cm^{2}h with constant current iontophoresis at 0.5 mA/cm^2 for 1 hour (Figure 2). This is comparable to numerous reports that state the advantages of pulsed DC or periodic iontophoresis over constant current delivery[16–18]. The pH of the skin surface (SC side) and receptor media was found to be unchanged at the end of the experiment (7.4–7.5), thus minimizing the chances of irritation and erythema in vivo studies. The stability of insulin in the receptor medium during the experiment was assessed by HPLC and no significant degradation was observed during iontophoresis.

It was noted that mDC iontophoresis alone failed to administer therapeutically relevant concentration of insulin [cumulative amount (t = 4 hours) = 0.863 ± 0.096 IU/cm^2]. Thus, various classes of CPEs including alcohols, fatty acids, bile salts, and terpenes were screened on porcine epidermis to study the permeation enhancement of insulin.

Enhancers augment the flux of peptides in conjunction with iontophoresis

Because the CPEs were applied on the surface as 5% ethanolic solutions, the effect of the solvents such as ethanol (EtOH) and propylene glycol (PG) on the barrier properties of the skin was studied. An increased flux was observed with EtOH as compared to passive application (0.098 ± 0.044 IU/cm^{2}h). However, with iontophoresis the increase in cumulative amount of insulin permeating

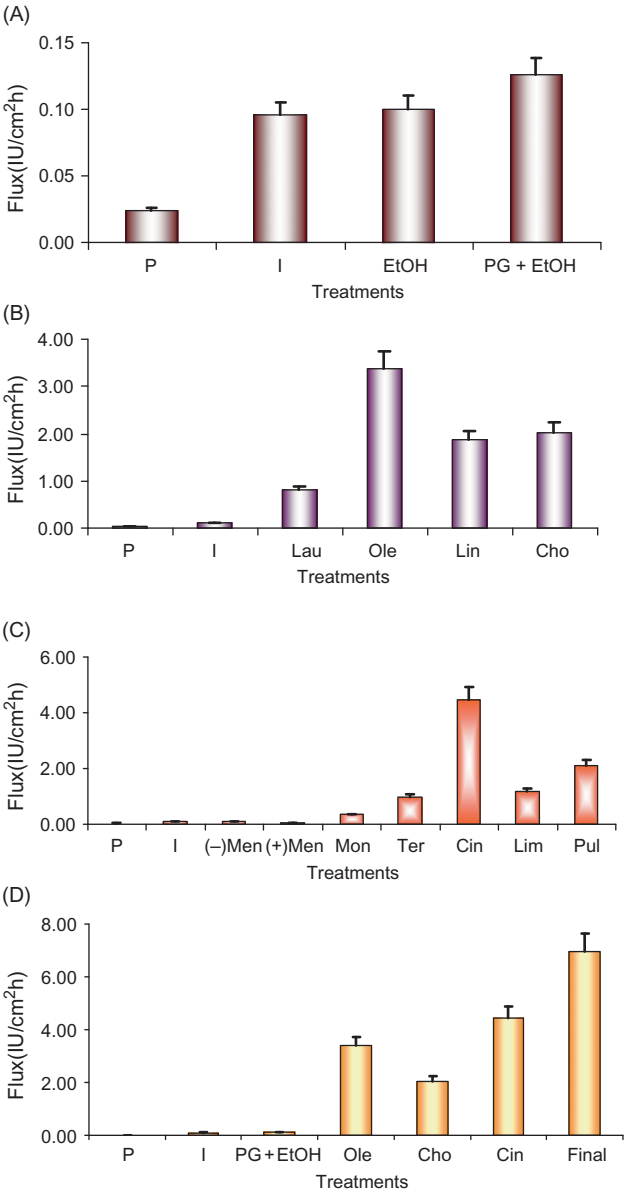

Figure 3. Comparison of insulin permeation profile on passive and pulsed iontophoresis with (A) solvents [P-Passive, I-Iontophoresis for 60 minutes, EtOH – ethanol, PG – propylene glycol], (B) 5% ethanolic solutions of terpenes [Mol – menthol, Mon – menthone, Ter – α-terpineol, Cin – cineole, Lim – limonene, Pul – pulegone, Ner – nerolidol], (C) 5% ethanolic solutions of fatty acids and bile salt (Ole-oleic acid, Lin-linoleic acid, Lau-lauric acid, Cho-sodium deoxycholate) pretreatment, and (D) combination (4 < n < 6 for all sets).

was slightly increased as compared with EtOH pretreatment alone (P > 0.05). However, addition of 70% PG to EtOH increased the dehydrating effects synergistically and high flux was obtained when combined with iontophoresis (0.126 ± 0.074 IU/cm^{2}h) (Figure 3A).

Application of a range of fatty acids consisting of oleic (Ole), linoleic, and lauric acids (5% solutions in EtOH) proved that C-18 was the optimum chain length

for effective permeation (enhancement ratio = 32.7 with Ole and 5.48 with lauric acid). Ole was found to have the highest flux both in passive application and in iontophoresis (0.145 ± 0.706 and 3.39 ± 1.20 IU/cm^{2}h, respectively; Figure 3B). No effect of increasing flux with unsaturation was observed. Additionally, the use of a bile salt, that is, sodium deoxycholate (Cho; 5% solution in EtOH), was found to enhance the permeation of insulin considerably on preapplication with iontophoresis (2.035 ± 0.465 IU/cm^{2}h). However, no effect was observed in the absence of iontophoresis.

Enhancement properties of both polar and nonpolar terpenes (1,8 cineole, α-terpineol, pulegone, nerolidol, menthone, (–)- and (+) menthol, and limonene) were investigated as 5% ethanolic solutions. In the presence as well as absence of iontophoresis, the highest insulin flux 4.453 ± 1.260 and 0.102 ± 0.014 IU/cm^{2}h, respectively, was achieved with 1,8 cineole (Cin) and was selected as a constituent of the final enhancer blend. The flux enhancement was in the following decreasing order: Cin > α-terpineol > pulegone > nerolidol > menthone > limonene > (–)menthol > (+) menthol (Figure 3C). Effect of stereospecificity on the permeation was also observed with menthol, in which the (–) isomer gave higher flux compared with (+) menthol in combination with iontophoresis (0.112 ± 0.047 and 0.063 ± 0.0087 IU/cm^{2}h, respectively).

Synergistic amplification of insulin flux with enhancer combination and iontophoresis

On the basis of the results obtained by individual enhancers, the effect of their combination was explored on porcine epidermis. The final enhancer combination consisting of 5% solutions of Ole, Cin, and Cho in PG : EtOH (7:3) was used for pretreatment (2 minutes) before application of the hydrogel patch. An increase in insulin flux was observed with 1 hour of mDC iontophoresis (5.12 ± 2.84 IU/cm^{2}h for porcine model, $P < 0.05$) compared with each of the CPEs alone. The high deviation in the flux is accountable to the difference in the fatty acid composition[19] and alteration in protein structure and epidermal thickness[20,21] because of aging as the skin samples could not be selectively screened into age groups because of limited availability.

Assessment of enhancer interactions by ATR–FTIR

Attenuated total reflectance (ATR)–FTIR spectrum of control cadaver epidermis showed asymmetric –CH_2 and –CH_3 stretching vibrations (υ_{asym}) at 2922.9 and 2955.5 cm^{-1} and symmetric vibrations (υ_{sym}) at 2852.5 and 2882.8 cm^{-1}, respectively. Characteristic amide I and II bands representing predominant α-structure of SC proteins were observed at 1642 and 1546 cm^{-1}, respectively. The amide I spectra were selected for assessment of the effects of various enhancers on the arrangement of proteins as it is well characterized into components corresponding to the varied conformational structures present[22]. Moreover, a change in the amide I bandwidth or bandshape suggests an alteration in the distribution of various secondary structure components or conformations[23]. Curve-fitting analysis of the control sample showed prevalence of helical structures (65.13%). Noticeable changes in the wavelengths, intensities, and peak parameters such as area of the above-mentioned vibrations were observed on CPE pretreatment suggesting changes in the lipid-protein packing of the epidermis (Tables 1 and 2; Figure 4a and b).

Lipid packing of SC is extensively altered by CPEs

EtOh and PG used as solvents for terpenes and fatty acids caused bathochromic shift of symmetric and asymmetric –CH_3 stretching vibrations. A massive change in the inter- and intrachain interactions was observed as a split in the –CH_3 υ_{asym} at 2955.5 cm^{-1} into 2968 and 2986 cm^{-1} on pretreatment with Cin. A similar observation was also reported on the application of Cho

Table 1. Comparison of curve-fitted infrared second-derivative spectra of lipid stretching vibrations from 2800–3000 cm^{-1}.

	Components			
	–CH_2		–CH_3	
Treatment (R^2)	υ_{sym} (% area)	υ_{asym} (% area)	υ_{sym} (% area)	υ_{asym} (% area)
Control (0.9955)	2852.5 (18.589)	2922.9 (54.927)	2882.8 (14.919)	2955.5 (11.563)
PG/EtOH (0.9937)	2851.6 (6.075)	2925.4 (48.392)	2876.2 (42.393)	2970.5 (3.138)
Cin* (0.9915)	2851.8 (14.547)	2921.8 (61.321)	2878.6 (17.454)	2968.0 (6.677)
				2986.0 (0.886)
Ole* (0.9943)	2852.6 (15.031)	2923.0 (54.909)	2874.8 (17.805)	2955.3 (12.252)
Cho* (0.9868)	2851.5 (17.825)	2921.1 (56.228)	2876.6 (20.932)	2973.5 (0.982)
				2982.7 (4.035)
Combination (0.9896)	2850.0 (4.847)	2920.2 (36.741)	2876.3 (51.630)	2969.4 (6.137)
		2937.0 (0.643)		

*All enhancers were used as 5% ethanolic solutions except PG, which was a 70% solution in EtOH.

Table 2. Comparison of curve-fitted infrared second-derivative spectra of Amide I vibration from 1600–1700 cm^{-1} of control sample with enhancer pretreatment.

		Components			
		Helices (%)			
Treatments (R^2)	Frequency (cm^{-1})	α	α'	Chain structures (%)	β-patterns (%)
Control (0.9993)	1642(*s*)	37.0741	28.0600	12.3094	22.5562
PG/EtOH (0.9959)	1651(*b*), 1627(*m*)	1.3586	56.3372	8.31592	33.9883
Cin* (0.9983)	1646(*s*)	1.2081	68.7187	19.4197	10.6533
Ole* (0.9991)	1645(*s*)	27.0893	29.3351	17.5356	26.0399
Cho* (0.9989)	1646(*s*)	26.3772	40.6033	4.69901	28.3204
Combination (0.9960)	1650(*s*), 1625(*s*)	1.2209	46.5718	19.3866	32.8205

s, strong; *m,* medium; *b,* broad; α, α-helix; α', irregular helix; chains, extended structures; β-patterns, antiparallel β-sheets and turns.
*All enhancers were used as 5% ethanolic solutions except PG, which was a 70% solution in EtOH.

(2955.5 $cm^{-1} \rightarrow$ 2973 and 2982 cm^{-1}) (Figure 4a; Table 1). This can be attributed to the unmasking of the end $-CH_3$ groups because of the lipid-extracting properties of the enhancers as well as because of the accumulation of the enhancers in the lipid layers. Further deposition was confirmed when the application of Cin showed pretreatment time-dependent derangement with broad features above 2971 cm^{-1} (1-hour pretreatment) resembling the stretching vibrations of the pure compound (data not shown). These peaks subsequently reduced in intensity on extensive washing for 12 hours, suggesting accumulation of Cin in the lipid bilayer. Ole application showed minor changes in the peak parameters and wavelength compared with other enhancers. Cho pretreatment also resulted in extensive reduction in all the vibrations with a maximum of 74.11% in the $-CH_3$ υ_{asym} (Table 1). The lateral crystal order ratio, a measure of inter- and intrachain interactions characterized by the ratio of υ_{asym} and υ_{sym} of the methylene groups, was found in the following order: PG > combination > Cin > Ole > control > Cho[24]. The reduction in the ratio on Cho pretreatment therefore suggests the stabilization of the lipid regions because of incorporation of the bulky sterol group. It is proposed that its interaction resembles that of cholesterol because of structural similarity thereby imparting rigidity to gel phase of lipid bilayer and reduced fluidity[25]. The high enhancement of 46.38% with Cin pretreatment observed in this diffusion study is supported by the increased chain interactions. It can be undoubtedly speculated from the curve-fitting analysis that the action of the enhancer combination is different from their individual effects. Splitting of the $-CH_2$ υ_{asym} from 2922.9 cm^{-1} into 2920.2 and 2937.0 cm^{-1} and decrease in the bandwidths of the methylene symmetric vibration by 38.96% suggest is loosening of the lipid packing and a high ratio of gauche conformers in the SC.

Enhancers cause conformational changes in SC proteins

X-ray diffraction studies have shown that the epidermis and SC proteins have a predominant α-helical conformation with 5–10% of another cross β-structure[26]. The conversion of $\alpha \rightarrow \beta$ has been reported on heat treatment of the tissue at 130°C in an autoclave for 1 hour[27]. A similar observation has also been observed on the treatment of SC with dimethyl sulfoxide in a study by Oertel[28]. It was postulated that an antiparallel β-sheet structure is formed by displacement of water molecules bound to the polar side chains of the protein resulting in the conversion of the α-helical part of the keratin filaments to β-structures. This process has, however, been claimed to be reversible, and decrease in the β-content was observed on rehydration and washing of dimethyl sulfoxide from the SC. Protein secondary conformations are characterized by narrow bands absorbing within specific regions of the amide I envelope: α-helix near 1649–1656 cm^{-1}, β-sheet near 1620–1635, 1670, and 1692–1697 cm^{-1}, and extended structures near 1645–1650 cm^{-1}[29–33]. In this study, pretreatment with CPEs resulted in rearrangement of the tightly packed α-helical structures into loosely arranged irregular helices with increase in extended chains, finally leading to the formation of β-patterns (Figure 4b). As the random coiled and α-regions show an overlap, it is difficult to assess the contributions of each to the formation of β-sheets.

The inset graph in Figure 4b shows the comparison of the ratios of various conformations present in the samples and their alterations on the application of enhancers. Pretreatment with PG : EtOH distorted the regular helical conformation with split in the amide I peak at 1642 cm^{-1} into 1651 and 1627 cm^{-1}. Approximately, 11% increment in the β-sheets was observed suggesting the loss of intramolecular H-bonds because of the dehydrating nature of the solvents. Application of Cin resulted in rearrangement of the α-helix to irregular

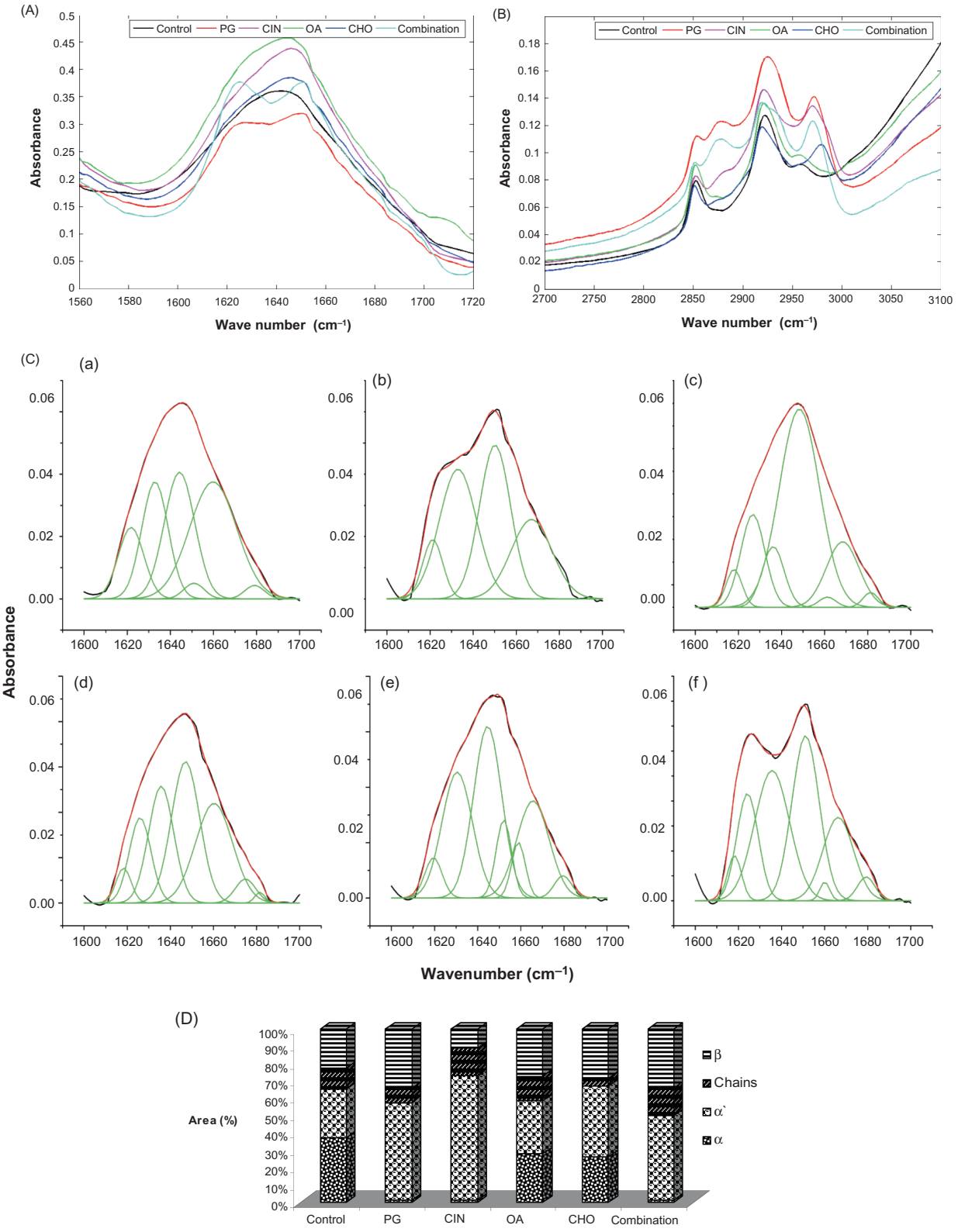

Figure 4. Comparison of infrared spectra of (A) lipid-stretching vibrations from 2700 to 3100 cm^{-1}, (B) amide I stretching vibrations from 1600 to 1720 cm^{-1} (PG – propylene glycol; CIN – cineole; OA – oleic acid; CHO – sodium deoxycholate), (C) curve-fitted inverted second derivative spectra of the amide I vibration between 1600 and 1700 cm^{-1}, (a) control; (b–f) pretreatment with PG/EtOH, cineole, oleic acid, sodium deoxycholate, and combination; and (D) comparison of various conformations (amide I) present in control sample and changes on pretreatment (α: α-helix; α': irregular helix; chains: extended structures; β: antiparallel β-sheets and turns).

helical structures and an increase in the extended chains implementing loosening of the fibrous keratin of the SC. As a contrary to the rest, Cin reduced the β-content by 11.90% (Table 2). It has been postulated that the increase in the β-components is responsible for the enhanced permeation across SC[28]. However, we have obtained considerably high flux with Cin pretreatment (4.453 ± 1.260 and 0.102 ± 0.014 IU/cm^{2}h in the presence and absence of iontophoresis, respectively), thereby warranting investigation of such an observation. On the basis of increasing β-content, the CPEs can be graded as Cin < control < Ole < Cho < combination < PG. The CPE combination showed an assimilation of the properties of the incorporated enhancers with an overall reduction in α-components by 17.342% (Table 2). The analysis therefore shows that it is the reduction in the α-contents resulting in slackening of the tightly packed SC that is responsible for the increase in permeation.

CLSM shows the localization of FITC-BI in the corneocyte envelopes of epidermis

CLSM was used to study the distribution of FITC-BI in cadaver epidermis at the cellular level. Artifacts because of the autofluorescence property of the skin were not observed at the selected wavelength (488 nm). Passive application of FITC-BI resulted in homogeneous distribution at the surface of SC with no differentiation in the cellular structures (Figure 5A). Extensive fluorescence was observed in wrinkles even after repeated washings.

Application of CPEs caused the concentration of the fluorescent probe at the corneocyte envelope (Figure 5B). Upon iontophoresis, FITC-BI was found to be concentrated around the hair follicle with some dilation. The corneocyte membranes were not clearly visible as with the enhancers (Figure 5C). Pretreatment followed by iontophoresis resulted in the accumulation of large amounts of FITC-BI in the deeper layers of the epidermis. As reported earlier, the follicle appeared extremely dilated proving the activation of shunt pathways in iontophoresis (Figure 5D). The honeycomb arrangement of epidermal cells with permeation of insulin by distinct paracellular pathways was noted even after 4 hours posttreatment (Figure 5E). High concentration of FITC-BI was also observed in the periphery of the hair follicle because of solubilization of the sebum present on the surface.

In vivo comparison of s.c. administration with transdermal iontophoresis with chemical pretreatment

A study was conducted to evaluate how s.c. administration can be correlated to transdermal delivery. Figure 6 shows the changes in %BGL upon various treatments with respect to the control group. It was found that s.c. injection showed an instantaneous lowering within 1 hour in %BGL by nearly 92% of the original values. The therapeutic activity was maintained for a period of 4–6 hours only. Thereafter, the glucose levels returned back to the original state. The blood glucose values were seen

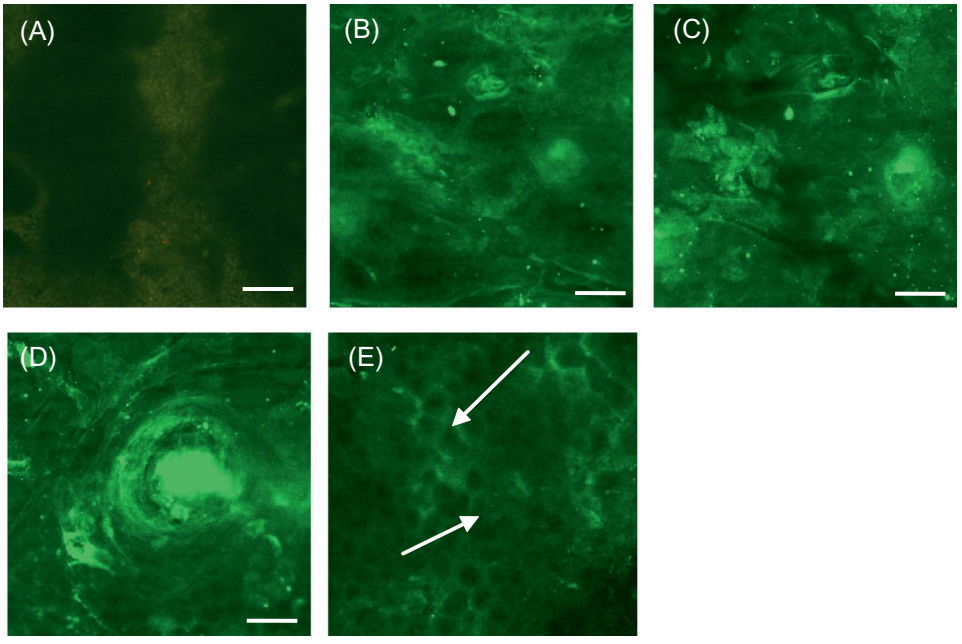

Figure 5. CLSM images of cadaver epidermis showing presence of FITC-BI on passive (A), enhancer without iontophoresis (B), iontophoresis, and (C) iontophoresis with enhancer pretreatment (D) and after 4 hours of treatment (E).

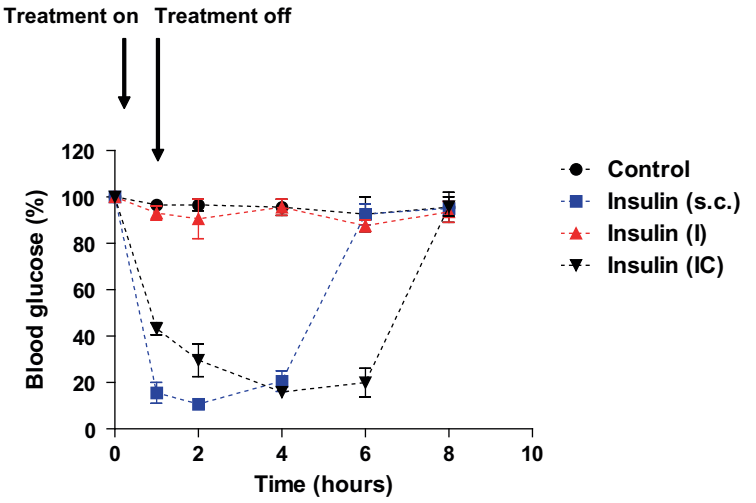

Figure 6. Reduction in %BGL upon insulin administration with respect to control treatment (s.c. = subcutaneous 30 IU/kg body weight, I = CPE pretreatment + 1-hour mDC iontophoresis, 0.5 mA/cm^2).

to fluctuate around that of the control group. On the contrary, iontophoresis alone failed to deliver insulin in vivo. Preapplication of enhancers followed by iontophoresis showed a prominent decline and recovery phase. Depression in %BGL by 28% was observed within 1 hour of application. The levels continued to fall exponentially with 45% decrease in BGL in the second hour and a maximum of 84% reduction at 4 hours postapplication (R^2 = 0.9791 for the decline phase). Thereafter, a gradual recovery toward the original status was noted. Blood glucose levels showed an exponential increase from 30% to 96% of the original values from 4 to 8 hours (R^2 = 0.9999, ANOVA, $P < 0.05$).

Discussion

The total insulin requirement in children and adults after diagnosis of Type 1 DM is in the range of 0.2–0.6 IU/kg body weight per day. Considering average weights of a child and an adult to be 20 and 70 kg, respectively, the amount of insulin required for daily administration ranges from 4 to 42 IU/day. Patients with C-peptide negative Type 1 DM need a further higher dosage of insulin in the range of 0.5–1 IU/day to maintain normoglycemic levels, amounting to a total of 35–70 IU/day[34]. Thus, it was targeted that the treatment strategy developed should be able to permeate a dose of around 5–10 IU/cm^{2}h to achieve desired insulin levels.

Earlier reports on insulin iontophoresis mention application of constant DC current for periods ranging from 2 to 7 hours, which cannot be practically applied in clinical settings[35,36]. In this setup, mDC sine iontophoresis (0.5 mA/cm^2 with 1 kHz frequency) was shown to be successful in delivering insulin by transdermal route. The treatment carried out for a maximum of 1 hour resulted in a fourfold increase (flux = 0.096 ± 0.040 IU/cm^{2}h) over constant current iontophoresis for the same current intensity and duration. Although the amount of insulin permeating was negligent compared with the desired targets stated above, the study throws light on the advantage of modulated iontophoresis over the conventional constant current protocols in reducing the duration of current administration. As modulated iontophoresis alone was not successful, effect of chemical pretreatment on permeation enhancement was studied.

Exploration of a range of CPEs with different chemical properties was carried out and a combination of 5% Cin, Ole, and Cho in PG : EtOH (7 : 3) was formulated. Application of 100 µL of the mixture on the SC followed by air-drying before iontophoresis yielded a maximum flux of 5.12 ± 2.84 IU/cm^{2}h showing an enhancement of 45-fold with respect to mDC iontophoresis alone. The action of enhancers is observed to be dependent on the properties of the molecule of interest as well as the in vitro model under experimentation. Pillai and Panchagnula[37,38] report maximum insulin permeation with neat menthone and lauric acid application in a set of separate experiments on rat skin. Permeation of zidovudine was, however, found to be the highest with 1,8 cineole pretreatment on rat skin[39]. A study of the effect of various enhancers by Rastogi and Singh[40] on insulin permeation across porcine epidermis showed 9.18- and 14.99-fold enhancement with linolenic acid and limonene, respectively, compared with iontophoresis alone[40].

It is thus reported that a combination of CPEs along with iontophoresis can deliver therapeutic levels of insulin. Currently, the data state permeation of nearly 7 IU of insulin per hour from 1 cm^2 area of the hydrogel

patch. Thus a mere increase in the patch area by a factor of 4 should be able to target the desired insulin level in patients requiring very high doses (1 IU/kg body weight) also. Based on the patient's requirement which is dependent on their diabetic status and carbohydrate intake, the hydrogel patches can be tailor-made. The amount of insulin incorporated per patch in this study was limited to 2 mg (57.2 IU) to avoid drug wastage, which can also be altered as per necessity.

To understand the synergistic effect of the selected CPEs, ATR–FTIR analysis of the treated samples was carried out and extensive alterations in the intensity and frequency of the lipid vibrations were observed. Cho has been used to increase permeation of peptides for conjunctival and nasal delivery[41,42]. However, its direct application as an enhancer for transdermal delivery has not been explored before. Being a surfactant in nature, it solubilizes both lipids and proteins thereby increasing the permeation of the peptide drug, insulin when combined with iontophoresis. It is hypothesized that the mechanism of interaction with lipid regions should be comparable to that of cholesterol because of structural similarity. This stabilization effect has been observed as a decrease in the frequency of the symmetric $-CH_3$ stretching vibration (7 cm^{-1}). It has been clearly observed in the study that the increased permeation with CPEs can be attributed to their lipid-disorganizing properties. Moreover, the proposed combination acts synergistically on the lipid regions causing increased ratio of gauche conformers and disorientation of the lamellar lipid phase. Changes in the amide I vibrations show a disruption of the H-bonds between the proteins and the lipid corneocyte envelopes thereby suggesting loosening of the keratinocytes and facilitation of the paracellular pathways. To further support the movement of insulin across the SC, pathways employed were traced using FITC-labeled insulin. This observation is also supported by the CLSM studies wherein accumulation of FITC-BI has found in the corneocyte envelopes even 4 hours after treatment. Extensive fluorescence around the hair follicle and the shaft also shows the solubilization of FITC-BI in the sebum, thereby promoting transfollicular uptake of the molecule. This clearly shows that the pathways created by only 2 minutes of CPE pretreatment and 1 hour of iontophoresis last for a considerable period of time. It therefore reflects that extensive pretreatment times ranging from 40 minutes to 2 hours reported in literature for insulin permeation are not required[35,43].

In vitro studies in our laboratory have shown permeation of nearly 7 IU of insulin per hour from ~2 cm^2 area of the hydrogel patch. Application of the same conditions in vivo resulted in gradual decrease with lowered blood glucose levels for a period of 8 hours proving the efficacy of the developed protocol.

Conclusions

To conclude, the work depicts the applicability of various enhancers in combination for enhancing the flux of large molecules such as insulin (5807.6 Da) to desired therapeutic levels. Perturbation of different vibration bands in the ATR–FTIR spectra suggests the varied sites of action of different classes of enhancers that have been synergistically exploited. This study is the first of its kind wherein the effects of more than one enhancer has been reported by second-derivative curve-fitting techniques. Both appendageal and paracellular pathways have been observed to play an important role in the permeation. Cross-sectional images of treated samples show that insulin has traversed not only the SC but also the epidermis with high fluorescent intensity in the dermal region. Post-chemical treatment of 1 hour of iontophoresis resulted in hypoglycemic conditions in diabetic rats for duration of 8 hours. Because the strategy applied in the experiment utilizes only 2 minutes of pretreatment time followed by 1-hour modulated iontophoresis, the combination can be of therapeutic benefit in the management of DM if proven through clinical trials in larger animals.

Acknowledgments

We thank Dr. S. Verma and Mr. B.D. Sharma, Institute of Pathology, New Delhi, India for their technical assistance in CLSM studies. The fellowship of R.R. was supported by Ranbaxy Research Foundation, Gurgaon, Haryana, India. The work has been supported by a project grant from the Department of Science and Technology, Government of India.

Declaration of interest

The authors report no conflicts of interest. The authors alone are responsible for the content and writing of this paper.

References

1. Naik A, Kalia YN, Guy RH. (2000). Transdermal drug delivery: Overcoming the skin's barrier function. Pharm Sci Technol Today, 3:318–26.
2. Barry BW. (2001). Novel mechanisms and devices to enable successful transdermal drug delivery. Eur J Pharm Sci, 14:101–14.
3. Gan D, ed. (2003). Diabetic atlas. 2nd ed. Brussels, Belgium: International Diabetes Federation.
4. King H, Rewers M. (1993). Global estimates for prevalence of diabetes mellitus and impaired glucose tolerance in adults. WHO ad hoc diabetes reporting group. Diabetes Care, 16:157–77.
5. Onkamo P, Vaananen S, Karvonen M, Tuomilehto J. (1999). Worldwide increase in incidence of Type I diabetes – the analysis

of the data on published incidence trends. Diabetologia, 42:1395–403.
6. Flood T. (2006). Advances in insulin delivery systems and devices: Beyond the vial and syringe. Insulin, 1:99–108.
7. Khafagy ES, Morishita M, Onuki Y, Takayama K. (2007). Current challenges in non-invasive insulin delivery systems: A comparative review. Adv Drug Deliv Rev, 59:1521–46.
8. Kligman AM, Chistophers E. (1963). Preparation of isolated sheets of human stratum corneum. Arch Dermatol, 88:702–5.
9. Joshi DP, Lan-Chun-Fung YL, Pritchard JG. (1979). Determination of poly (vinyl alcohol) via its complex with boric acid and iodine. Anal Chim Acta, 104:153–60.
10. Banga AK, Chien YW. (1993). Hydrogel based iontotherapeutic delivery device for transdermal delivery of peptide/protein drugs. Pharm Res, 10:697–702.
11. Anand S, Koul V, Rastogi R. (2006). Modulated DC iontophoretic device. Ind. patent application 710/DEL/2006.
12. Scheuplein RJ. (1978). Skin as barrier. In: Jarret A, ed. The physiology and pathophysiology of skin. New York: Academic Press, 1693–730.
13. Junod A, Lambert AE, Stauffacher W, Renold AE. (1969). Diabetogenic action of streptozotocin: Relationship of dose to metabolic response. J Clin Invest, 48:2129–39.
14. Davies DJ, Ward RJ, Heylings JR. (2004). Multi-species assessment of electrical resistance as a skin integrity marker for in vitro percutaneous absorption studies. Toxicol In Vitro, 18:351–8.
15. Wester RC, Maibach HI. (1989). In vivo animal models for percutaneous absorption. In: Bronaugh RL, Maibach HI, eds. Percutaneous absorption, mechanisms–methodology–drug delivery. New York: Marcel Dekker, 221–38.
16. Craane-van-Hinsberg WHM, Bax L, Flinterman NHM, Verhoef J, Junginger HE, Bodde HE. (1994). Iontophoresis of a model peptide across human skin in vitro: Effects of iontophoresis protocol, pH, and ionic strength on peptide flux and skin impedance. Pharm Res, 11:1296–300.
17. Raiman J, Koljonen M, Huikko K, Kostiainen R, Hirvonen J. (2004). Delivery and stability of LHRH and nafarelin in human skin: The effect of constant/pulsed iontophoresis. Eur J Pharm Sci, 21:371–7.
18. Prasad R, Koul V, Anand S, Khar RK. (2007). Effect of DC/mDC iontophoresis and terpenes on transdermal permeation of methotrexate: In vitro study. Int J Pharm, 333:70–8.
19. Nazzaro-Porro M, Passi S, Boniforti L, Belsito F. (1979). Effects of aging on fatty acids in skin surface lipids. J Invest Dermatol, 73:112–7.
20. Sauermann K, Clemann S, Jaspers S, Gambichler T, Altmeyer P, Hoffmann K, et al. (2002). Age related changes of human skin investigated with histometric measurements by confocal laser scanning microscopy in vivo. Skin Res Technol, 8:52–6.
21. Bhattacharyya TK, Thomas JR. (2004). Histomorphologic changes in aging skin, observations in the CBA mouse model. Arch Facial Plast Surg, 6:21–5.
22. van de Weert M, Haris PI, Hennink WE, Crommelin DJA. (2001). Fourier transform infrared spectrometric analysis of protein conformation: Effect of sampling method and stress factors. Anal Biochem, 297:160–9.
23. Goates CY, Knutson K. (1994). Enhanced permeation of polar compounds through human epidermis. I. Permeability and membrane structural changes in the presence of short chain alcohols. Biochim Biophys Acta, 1195:169–79.
24. Bunow MR, Levin IW. (1977). Comment on the carbon-hydrogen stretching region of vibrational Raman spectra of phospholipids. Biochim Biophys Acta, 487:388–94.
25. Raffy S, Teissié J. (1999). Control of lipid membrane stability by cholesterol content. Biophys J, 76:2072–80.
26. Baden HP, Bonar L, Katz E. (1968). The fibrous protein of epidermis. J Invest Dermatol, 50:301–5.
27. Baden HP, Goldsmith LA, Bonar L. (1973). Conformational changes in the α-fibrous protein of epidermis. J Invest Dermatol, 60:215–8.
28. Oertel RP. (1977). Protein conformational changes induced in human stratum corneum by organic sulfoxides: An infra-red spectroscopic investigation. Biopolymers, 16:2329–45.
29. Byler DM, Susi H. (1986). Examination of the secondary structure of proteins by deconvolved FTIR spectra. Biopolymers, 25:469–87.
30. Bendit EG. (1966). Infrared absorption spectrum of keratin. I. Spectra of α-, β-, and supercontracted keratin. Biopolymers, 4:539–59.
31. Chirgadze YN, Shestopalov BV, Venyaminov SY. (1973). Intensities and other spectral parameters of infrared amide bands of polypeptides in the beta- and random forms. Biopolymers, 12:1337–51.
32. Tatulian SA. (2003). ATR-FTIR: A method of choice for studying membrane proteins and lipids. Biochemistry, 42:11898–907.
33. Khurana R, Fink AL. (2000). Do parallel β-helix proteins have a unique Fourier transform infrared spectrum? Biophys J, 78:994–1000.
34. Hirsch IB. (1999). Type 1 diabetes mellitus and the use of flexible iInsulin regimens. Am Fam Physician, 60:2343–56.
35. Pillai O, Nair V, Poduri R, Panchagnula R. (1999). Transdermal iontophoresis. Part II: Peptide and protein delivery. Methods Find Exp Clin Pharmacol, 21:229–41.
36. Chien YW, Siddiqui Y, Sun Y, Shi WM, Liu JC. (1987). Transdermal iontophoretic delivery of therapeutic peptides/proteins (I) Insulin. In: Juliano RL, ed. Biological approaches in controlled delivery of drugs. Ann NY Acad Sci, 507:32–50.
37. Pillai O, Panchagnula R. (2003). Transdermal iontophoresis of insulin V. Effect of terpenes. J Control Release, 88:287–96.
38. Pillai O, Panchagnula R. (2004). Transdermal iontophoresis of insulin. VI. Influence of pretreatment with fatty acids on permeation across rat skin. Skin Pharmacol Physiol, 17:289–97.
39. Narishetty STK, Panchagnula R. (2004). Transdermal delivery of zidovudine: Effect of terpenes and their mechanism of action. J Control Release, 95:367–79.
40. Rastogi SK, Singh J. (2005). Effect of chemical penetration enhancer and iontophoresis on the in vitro percutaneous absorption enhancement of insulin through porcine epidermis. Pharm Dev Technol, 1:97–104.
41. Hayakawa E, Chien DS, Inagaki K, Yamamoto A, Wang W, Lee VHL. (1992). Conjunctival penetration of insulin and peptide drugs in the albino rabbit. Pharm Res, 9:769–75.
42. Johansson F, Hjertberg E, Eirefelt S, Tronde A, Bengtsson UH. (2002). Mechanisms for absorption enhancement of inhaled insulin by sodium taurocholate. Eur J Pharm Sci, 17:63–71.
43. Rastogi SK, Singh J. (2002). Transepidermal transport enhancement of insulin by lipid extraction and iontophoresis. Pharm Res, 19:427–33.